Electronic Supplementary Material (ESI) for Environmental Science: Nano.

Supporting Information

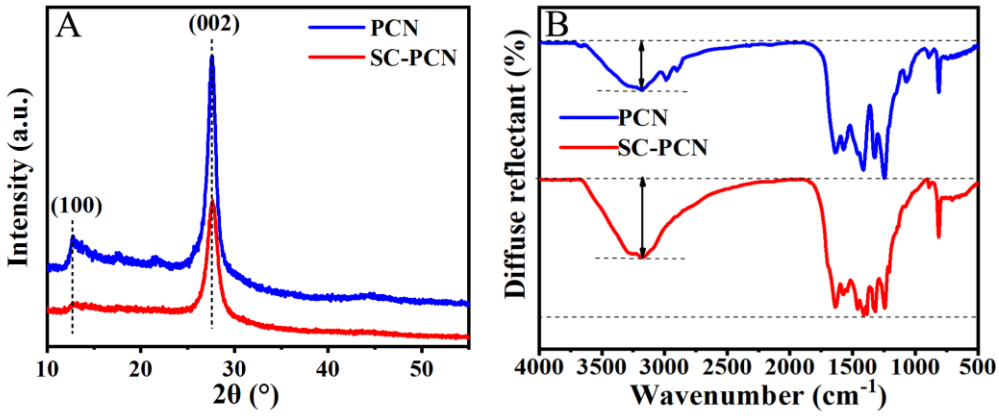

Fig. S1 XRD (A) and FT-IR (B) spectra of the PCN and SC-PCN.

Table S1 BET surface areas and corresponding pore sizes of different synthetic processes

Samples	Processing step	BET Surface Area ($m^2 g^{-1}$)	Pore Size (nm)
1	Primary PCN	171.7	7.3
2	PCN treated with HNO_3	74.2	8.5
3	Primary SC-PCN	222.3	9.6
4	SC-PCN treated with HNO_3	177.8	8.8
5	SC-PCN with HNO_3 pretreatment	178.0	8.9

Table S2 Organic elemental analysis of g-C_3N_4 with different treating processes

Sample	C(wt%)	N(wt%)	O(wt%)	H(wt%)
Primary PCN	34.51	59.42	4.39	1.68
Primary SC-PCN	33.92	58.60	5.67	1.81
SC-PCN treated with HNO_3	30.67	55.08	11.94	2.31

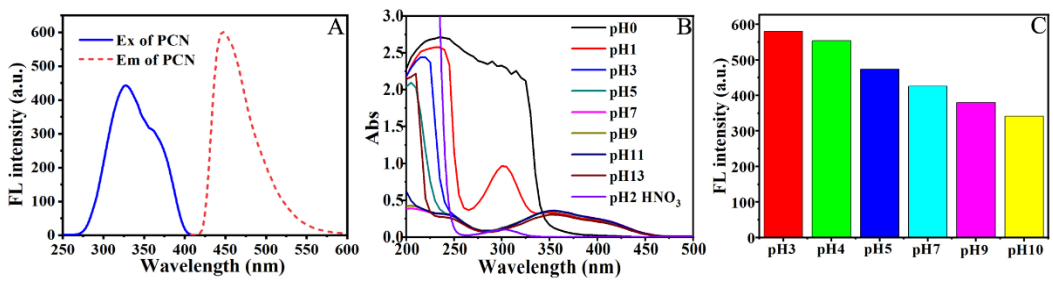

Fig. S2 (A) Fluorescence spectra of excitation and emission PCN. (B) UV-vis absorption spectra of HNO_3 and TNP in different pH values. (C) Fluorescence intensities of PCN in different pH values.

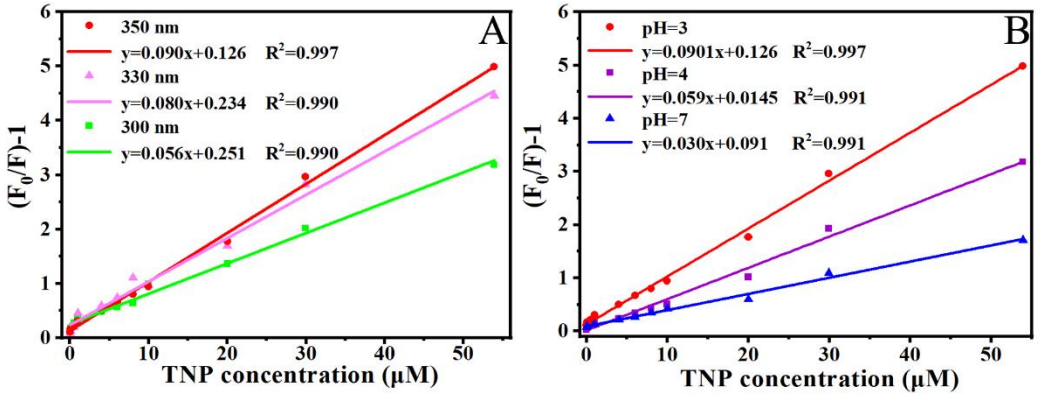

Fig. S3 (A) Fluorescence determination of TNP by PCN in pH 3 with linearity range from 0.01 to 54 μM at excitation wavelength of 300, 330 and 350 nm. (B) Fluorescence determination of TNP by PCN in different pH solutions (pH=3, 4 and 7) with linearity range from 0.01 to 54 μM with excitation wavelength of 350 nm.

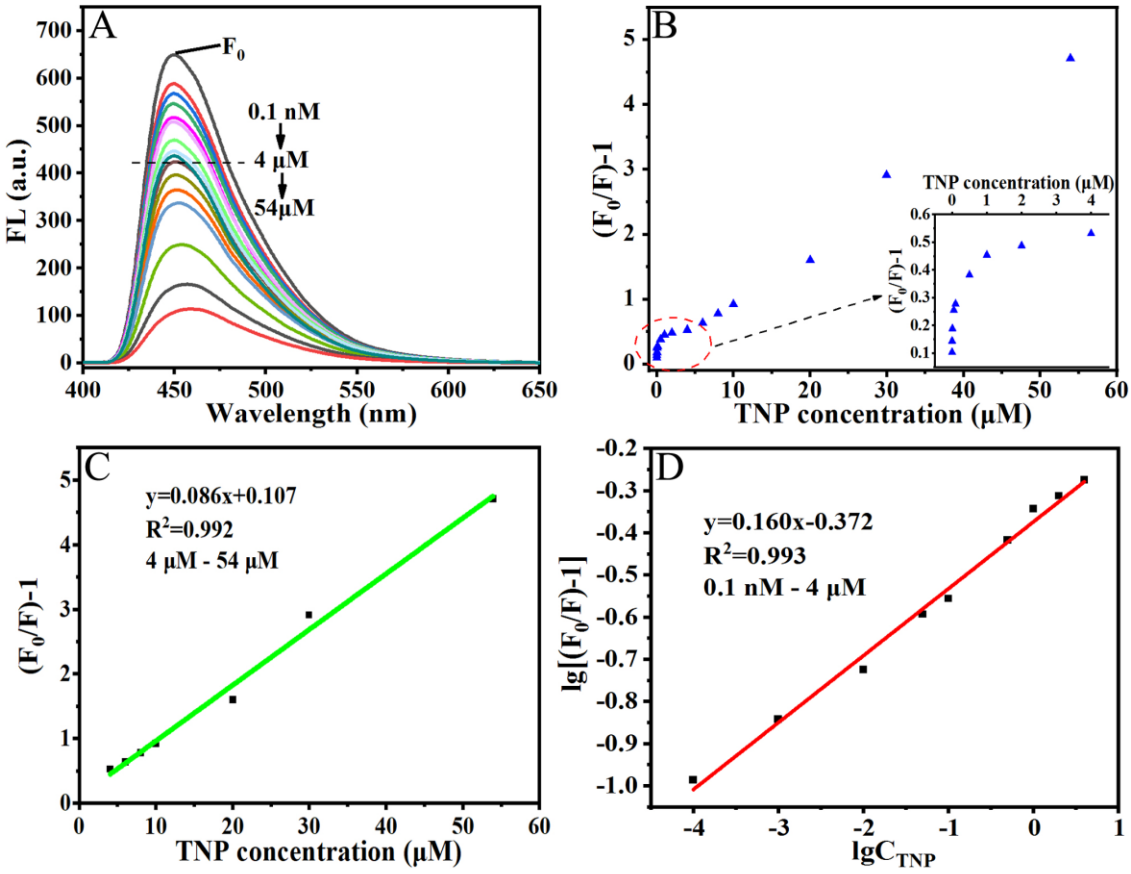

Fig. S4 (A) The fluorescence spectra of SC-PCN in the presence of different concentrations of TNP in pH 7 (0.0001, 0.001, 0.01, 0.05, 0.1, 0.5, 1, 2, 4, 6, 8, 10, 20, 30, and 54 μM). (B) Fluorescence determination of TNP by SC-PCN in pH 7, with the magnification of determination for 0.1 nM-4 μM as the inset. (C) Fluorescence determination of TNP by SC-PCN with linearity ranges from 4 to 54 μM by normal SVE. (D) Fluorescence determination of TNP by SC-PCN with linearity ranges from 0.1 nM to 4 μM by double logarithmic fitting of $\boldsymbol{lg[(F_0/F)-1]}$ and $\boldsymbol{lgC_{TNP}}$.

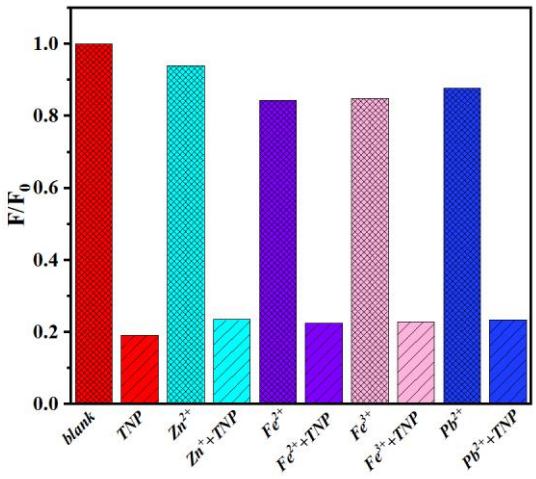

Fig. S5 Fluorescence response of the SC-PCN in the presence of 10 μM TNP and other co-existing metal ions. F_0 and F represent the fluorescence intensity of SC-PCN in the absence and presence of TNP and other metal ions.

Table S3 Parameters of adsorption kinetics fits for TNP adsorption

Adsorbent	Temperature	Pseudo-second-order kinetics			
		Equation	Q_e (mg g^{-1})	k_2 (g mg^{-1} min^{-1})	R^2
SC-PCN	room temperature	y=0.0153x+0.00159	65.49	0.15	0.997
PCN	room temperature	y=0.0179x+0.0414	55.99	0.0077	0.998

Table S4 Parameters of Henry, Freundlich fits for TNP adsorption

Sample	Henry		Freundlich			Henry- Freundlich				
						Henry (0-0.87 μM)		Freundlich (0.87-44 μM)		
	K_h (L g^{-1})	R^2	K_F (L g^{-1})	N	R^2	K_h (L g^{-1})	R^2	K_F (L g^{-1})	N	R^2
SC-PCN	4.3661	0.964	8.68	1.19	0.9776	18.611	0.9999	10.77	1.58	0.9957
PCN	3.1399	0.9961	3.88	1.06	0.9987	--				

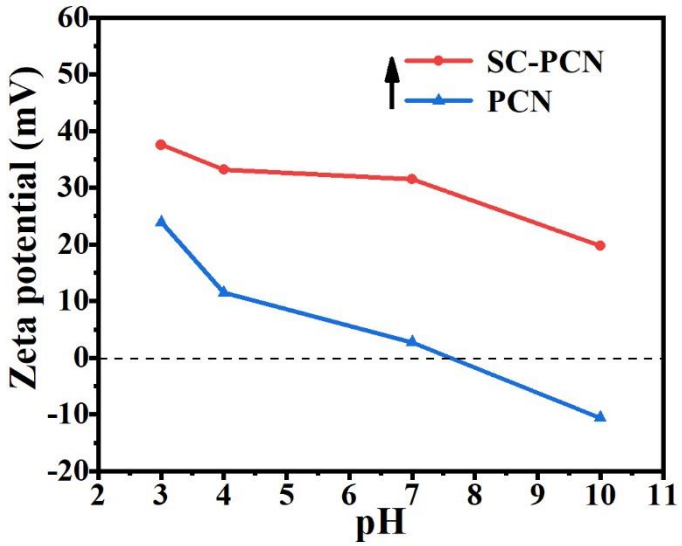

Fig. S6 Zeta potential measurements in different pH solutions by PCN and SC-PCN.

Table S5 Determination of TNP spiked in water samples (n=6)

Water samples	Concentration added (μM)	Concentration found (μM)	Recovery (%)[a]	RSD (%)
Sample 1	0.02	0.0236	118.0	10.03
	1	0.946	94.6	5.62
	10	10.080	100.8	2.39
Sample 2	0.02	0.0231	115.5	11.18
	1	1.051	105.1	5.75
	10	10.020	100.2	2.48
[a] Recovery (%)= 100 × (concentration found/concentration added).				

Table S6 Performance comparison with other reported methods for TNP sensing

Methods	Linear detection range	Detection limit	Water samples	Reference
Silicon nanoparticles(SiNPs)	0.087 -- 523 μM	29 nM	River and tap water	7
Chemically oxidized and liquid exfoliated g-C_3N_4 nanosheets	0 -- 0.5 μM 0.5 -- 10 μM	8.2 nM	Lake water and sea water	17
Terbium-doped blue carbon dots	500 nM -- 100 μM	200 nM	Running water and lake water	10
Fluorescence quantum dots ZnS:Mn^{2+}@allyl mercaptan (QDs@AM)	0.22 -- 35 μM	3.4nM	Lake water	S1
Cd-Metal–Organic	0 -- 40 μM	1.3μM	--	9
Fluorescent method with	0.218 -- 305 μM	0.141 μM	--	S2

8-hydroxyquinoline Aluminum nanospheres				
Fluorescent method with MoS_2 quantum dots	0.099 -- 36.5 μM	95 nM	Lake water	6
Carbon dots	0 -- 30 μM	75.6 nM	--	S3
Fluorescent method with phosphonated pyrene derivatives	0 -- 35 μM	61nM	--	S4
Luminescent graphene quantum dots (GQDs)	1 -- 60 μM	0.3 μM	Lake water	S5
Zn(II)/Cd(II) mixed ligand coordination polymers (CPs)	0 -- 0.2 mM	0.06 μM	--	S6
Co(II)/Cd(II) Metal Organic Frameworks		0.15μM	---	S7
Boron nitride quantum dots (BNQDs).	0.25 -- 200 μM	0.14 μM	River water	S8
Rotational paper-based microfluidic chips (RPADs)	17.2 -- 87.3 μM	0.31μM	Lake and sea water	S9
Hydrazine-substituted BODIPY probe	0 -- 40 μM,	0.44 μM	--	S10
This work	0.1 nM -- 4 μM 4 μM -- 54 μM	0.04 nM	Ground water and lake water	

S1 M. Bai, S. N. Huang, S. Y. Xu, G. F. Hu and L. Y. Wang, Fluorescent nanosensors via photoinduced polymerization of hydrophobic inorganic quantum dots for the sensitive and selective detection of nitroaromatics, *Anal. Chem.,* **2015**, 87, 2383−2388.

S2 Y. X. Ma, H. Li, S. Peng and L. Y. Wang, Highly selective and sensitive fluorescent paper sensor for nitroaromatic explosive detection, *Anal. Chem.*, **2012**, 84, 8415−8421.

S3 S. Md Palashuddin and C. Arun, Induction coil heater prepared highly fluorescent carbon dots as invisible ink and explosive sensor, *RSC Adv.,* **2014**, 4, 31994-31999.

S4 N. Venkatramaiah, A. D. G. Firmino, F. A. Almeida Paz and J. P. C. Tomé, Fast detection of nitroaromatics using phosphonate pyrene motifs as dual chemosensors, *Chem.Commun.,* **2014**, *50*, 9683-9686.

S5 L. P. Lin, M. C. Rong, S. S. Lu, X. H. Song, Y. X. Zhong, J. W. Yan, Y. R. Wang, X. Chen, A facile synthesis of highly luminescent nitrogen-doped graphene quantum dots for the detection of 2,4,6-trinitrophenol in aqueous solution, *Nanoscale*, **2015**, 7, 1872–1878.

S6 B. Parmar, Y. Rachuri, K. K. Bisht, R. Laiya and E. Suresh, Mechanochemical and conventional synthesis of Zn(II)/Cd(II) luminescent coordination polymers: dual sensing probe for selective detection of chromate anions and TNP in aqueous phase, *Inorg. Chem.*, **2017**, 56, 2627−2638.

S7 Y. Rachuri, B. Parmar and E. S. Cryst, Three-dimensional Co(II)/Cd(II) metal−organic frameworks:luminescent Cd-MOF for detection and adsorption of 2,4,6-trinitrophenol in the aqueous phase, *Growth Des.*, **2018**, 18, 3062−3072.

S8 D. Peng, L. Zhang, F. F. Li, W. R. Cui, R. P. Liang and J. D. Qiu, Facile and green approach to the synthesis of boron nitride quantum dots for 2,4,6-trinitrophenol sensing, *ACS Appl. Mater. Interfaces*, **2018**, 10, 7315−7323.

S9 J. Qi, B. W. Li, X. Y. Wang, L. W. Fu, L. Q. Luo and L. X. Chen, Rotational paper-based microfluidic-chip device for multiplexed and simultaneous fluorescence detection of phenolic pollutants based on a

molecular-imprinting technique, *Anal. Chem.*, **2018**, 90, 11827−11834.

S10 J. M. Gao, X. X. Chen, S. Q. Chen, H. Meng, Y. Wang, C. S. Li and L. Feng, The BODIPY-based chemosensor for fluorometric/colorimetric dual channel detection of RDX and PA, *Anal. Chem.*,**2019**, DOI:10.1021/acs.analchem.9b02888.